JHEP PROCEEDINGS

Trieste Meeting of the TMR Network on Physics beyond the SM

A consistent approach to bubble-nucleation theory

N. Tetradis*

Scuola Normale Superiore, Piazza dei Cavalieri 7, Pisa 56126, Italy
E-mail: tetradis@cibs.sns.it

Abstract: We summarize recent work on the consistent calculation of bubble-nucleation rates. Our approach is based on the notion of a real coarse-grained potential. The bubble-nucleation rate is calculated through an expansion around the semiclassical saddle point associated with tunnelling. We resolve outstanding problems related to the convexity of the potential, the double-counting of the effect of fluctuations and the inherent ultraviolet divergences. We determine the region of validity of the expansion around the saddle point. We find that this expansion fails near the spinodal line, and for weak or radiatively induced first-order phase transitions. We apply our method to the bound on the Higgs-boson mass from vacuum metastability and the electroweak phase transition.

Developing a consistent theory of bubble nucleation is an important problem for particle and statistical physics. Possible applications include the description of most cosmological phase transitions, the questions of tunnelling in quantum mechanics and field theory, the problem of vacuum stability and its phenomenological consequences, the (currently unsatisfactory) explanation of the experimentally measured bubble-nucleation rates for statistical systems, etc. The estimates of bubble-nucleation rates for first-order phase transitions are usually carried out within Langer's theory of homogeneous nucleation [1], applied to relativistic field theory in refs. [2]. The nucleation rate is exponentially suppressed by the action (free energy rescaled by the temperature) of the critical bubble, a saddle point of the free energy of the system. Significant contributions to the nucleation rate may arise from higher orders in a systematic expansion around this saddle point. The first correction has the form of a pre-exponential factor that involves fluctuation determinants around the critical bubble and the false vacuum. The evaluation of this factor is a difficult problem at the conceptual and technical level, as crucial issues associated with the convexity of the potential, the divergences of the fluctuation determinants and the double-counting of the effect of fluctuations must be resolved.

*Report on work done in collaboration with A. Strumia and C. Wetterich.

1. The method

In a series of recent works [3]–[7], following the proposal of refs. [8], we developed a consistent approach, based on the effective average action Γ_k [9] that can be interpreted as a coarse-grained free energy. Fluctuations with characteristic momenta larger than a coarse-graining scale ($q^2 \gtrsim k^2$) are integrated out and their effect is incorporated in Γ_k. In the limit $k \to 0$, Γ_k becomes the effective action. The k dependence of Γ_k is described by an exact flow equation [10]. This can be translated into evolution equations for functions appearing in a derivative expansion of the action [11]. An approximation that is sufficient in many cases takes into account the effective average potential U_k and a standard kinetic term and neglects higher derivative terms in the action. The bare theory is defined at some high scale Λ that can be identified with the ultraviolet cutoff. It is, however, more convenient to choose a starting scale k_0 below the temperature T, where the effective average action of a $(3+1)$-dimensional theory at non-zero temperature can be described in terms of an effective three-dimensional action at zero temperature [12].

In ref. [3] we computed the form of U_k at scales $k \leq k_0$ for a theory of one scalar field by integrating its evolution equation [10, 11]

$$\frac{\partial}{\partial k^2} U_k(\phi) = -\frac{1}{8\pi} \mathrm{Tr} \sqrt{k^2 + U_k''(\phi)}. \qquad (1.1)$$

We considered an initial potential U_{k_0} with two minima separated by a barrier. U_k is real and non-convex for non-zero k, and approaches convexity only in the limit $k \to 0$. The nucleation rate must be computed for k larger than the scale k_f for which the negative curvature at the top of the barrier becomes approximately equal to $-k_f^2$ [13]. For $k < k_f$ the form of the potential is affected by field configurations that interpolate between the two minima (similar to critical bubbles). For $k \gtrsim k_f$ the typical length scale of a thick-wall critical bubble is $\gtrsim 1/k$.

We performed the calculation of the nucleation rate for a range of scales above and near k_f. The nucleation rate is given by

$$I = A_k \exp(-S_k),$$

where

$$A_k = \frac{E_0}{2\pi} \left(\frac{S_k}{2\pi}\right)^{3/2} \left| \frac{\mathrm{Det}' \left[-\partial^2 + U_k''(\phi_b(r))\right]}{\mathrm{Det}\left[-\partial^2 + k^2 + U_k''(\phi_b(r))\right]} \times \right.$$

$$\left. \times \frac{\mathrm{Det}\left[-\partial^2 + k^2 + U_k''(0)\right]}{\mathrm{Det}\left[-\partial^2 + U_k''(0)\right]} \right|^{-1/2}. \qquad (1.2)$$

Here $\phi_b(r)$ is the profile of the spherically symmetric saddle point, S_k its action determined by using the potential $U_k(\phi)$, and $\phi = 0$ corresponds to the false vacuum. The prime in the fluctuation determinant around the saddle point denotes that the 3 zero eigenvalues of the operator $-\partial^2 + U_k''(\phi_b(r))$, corresponding to displacements of the critical bubble, have been removed. E_0 is the square root of the absolute value of the unique negative eigenvalue. The above form of A_k guarantees that only modes with characteristic momenta $q^2 \lesssim k^2$ contribute to the nucleation rate. (The effect of modes with $q^2 \gtrsim k^2$ is already incorporated in the form of $U_k(\phi)$.) We emphasize that the use of an ultraviolet cutoff in eq. (1.2) that matches the infrared cutoff procedure in the derivation of eq. (1.1) is crucial for the consistency of our approach. In both cases, mass-like cutoffs have been used.

2. Typical calculations

The details of the numerical evaluation of the complicated determinants in eq. (1.2) are given in ref. [3]. Fig. 1 exhibits the results of the calculation for an initial potential

$$U_{k_0}(\phi) = \frac{1}{2} m_{k_0}^2 \phi^2 + \frac{1}{6} \gamma_{k_0} \phi^3 + \frac{1}{8} \lambda_{k_0} \phi^4 \qquad (2.1)$$

that has a form typical for first-order phase transitions in four-dimensional field theories at high temperature. Through a shift $\phi \to \phi + c$ the cubic term can be eliminated in favour of a term linear in ϕ. Therefore, eq. (2.1) also describes statistical systems of the Ising universality class in the presence of an external magnetic field. The first row corresponds to parameters $m_{k_0}^2 = -0.0433\ k_0^2$, $\gamma_{k_0} = -0.0634\ k_0^{3/2}$, $\lambda_{k_0} = 0.1\ k_0$. The first plot shows the evolution of the potential $U_k(\phi)$ as the scale k is lowered. (We always shift the metastable vacuum to $\phi = 0$.) The solid line corresponds to $k/k_0 = 0.513$ while the line with longest dashes (that has the smallest barrier height) corresponds to $k_f/k_0 = 0.223$. At the scale k_f the negative curvature at the top of the barrier is slightly larger than $-k_f^2$ and we stop the evolution. The potential and the field have been normalized with respect to k_f. As k is lowered from k_0 to k_f, the absolute minimum of the potential settles at a non-zero value of ϕ, with a significant barrier separating it from the metastable minimum at $\phi = 0$. The second plot displays the profile of the saddle point $\phi_b(r)$ in units of k_f for the same sequence of scales. For $k \simeq k_f$ the characteristic length scale of the bubble profile and $1/k$ are comparable. This is an indication that we should not proceed to coarse-graining scales below k_f.

Our results for the nucleation rate are presented in the third plot. The horizontal axis corresponds to $k/\sqrt{U_k''(\phi_t)}$, i.e. the ratio of the scale k to the mass of the field at the absolute minimum located at ϕ_t. Typically, when k crosses below this mass, the massive fluctuations of the field start decoupling. The evolution of the convex parts of the potential slows down and eventually stops. The dark diamonds give the values of the action S_k (free energy rescaled by the temperature) of the saddle point at the scale k.

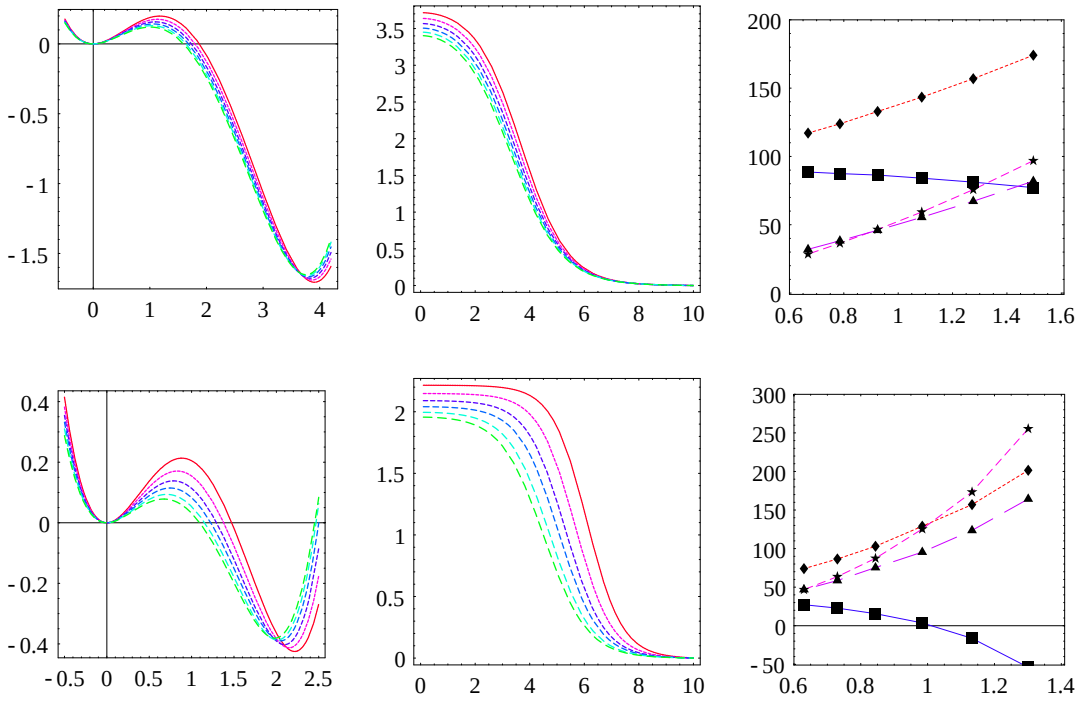

Figure 1: Dependence of potential $U_k(\phi)$, critical bubble $\phi_b(r)$ and nucleation rate I/k_f^4 on the coarse graining scale k. The initial potential is given by eq. (2.1) with $\lambda_{k_0} = 0.1 \cdot k_0$, $m^2_{k_0} = -0.0433 \cdot k_0^2$, $\gamma_{k_0} = -0.0634\ k_0^{3/2}$ (first row) and $\lambda_{k_0} = 0.1 \cdot k_0$, $m^2_{k_0} = -0.013 \cdot k_0^2$, $\gamma_{k_0} = -1.61 \cdot 10^{-3}\ k_0^{3/2}$ (second row).

We observe a strong k dependence of this quantity. The stars indicate the values of $\ln(A_k/k_f^4)$. Again a substantial decrease with decreasing k is observed. This is expected, because the fluctuation determinants in A_k are calculated with an effective ultraviolet cutoff of order k. The dark squares give our results for $-\ln(I/k_f^4) = S_k - \ln(A_k/k_f^4)$. The k dependence of this quantity almost disappears for $k/\sqrt{U_k''(\phi_t)} \lesssim 1$. The small residual dependence on k can be used in order to estimate the effect of the next order in the expansion around the saddle point. This contribution is expected to be smaller than $\ln(A_k/k_f^4)$. It is apparent from fig. 1 that the leading contribution to the pre-exponential factor increases the total nucleation rate. This behaviour, associated with the fluctuations of the field whose expectation value serves as the order parameter, is observed in multi-field models as well.

Our results confirm the expectation that the nucleation rate should be independent of the scale k that we introduced as a calculational tool. They also demonstrate that all the configurations of the second plot give equivalent descriptions of the system, at least for the lower values of k. This indicates that the critical bubble should not be associated only with the saddle point of the semi-classical approximation, whose action is scale dependent. Only the combination of the saddle point and its possible deformations in the thermal bath has physical meaning.

For larger values of $\lambda_{k_0}/(-m^2_{k_0})^{1/2}$ the dependence of the nucleation rate on k becomes more pronounced. We demonstrate this in the second row of plots, for which $\lambda_{k_0} = 0.1 \cdot k_0$, $m^2_{k_0} = -0.013 \cdot k_0^2$, $\gamma_{k_0} = -1.61 \cdot 10^{-3}\ k_0^{3/2}$ and $k_f/k_0 = 0.0421$. The dimensionless coupling is $\lambda_{k_0}/(-m^2_{k_0})^{1/2} = 0.88$ (instead of 0.48 for the first row). The first-order contribution $\ln(A_k/k_f^4)$ in the expansion around the saddle point is now comparable to the lowest order contribution S_k. This indicates that higher orders in the expansion are important and the series stops converging. Therefore, there is a limit to the validity of Langer's theory of homogeneous nucleation.

3. Validity of the theory of homogeneous nucleation

An intuitive derivation of the region of applicability of this theory can be obtained through use of approximate analytical expressions for the pre-exponential factor. The dark triangles in the third plot of each row in fig. 1 display values predicted by the approximate expression [4, 7]

$$\ln \frac{A_k}{k^4} \approx \frac{\pi k}{2} \left[- \int_0^\infty r^3 \left[U_k'' \left(\phi_b(r) \right) - U_k'' \left(0 \right) \right] dr \right]^{1/2}. \tag{3.1}$$

Good agreement is observed with the numerical results denoted by stars, especially in the first case in which the expansion around the saddle point converges.

Let us consider a potential given by eq. (2.1), with $m_{k_0}^2 > 0$[1]. As the bubble-nucleation rate is largely independent of k when homogeneous nucleation theory is applicable, we can obtain an estimate of the rate by using $k = k_0$ and eq. (3.1). Through appropriate rescalings of r and ϕ we can define a dimensionless potential $\tilde{U}(\tilde{\phi}) = \tilde{\phi}^2/2 - \tilde{\phi}^3/3 + h\,\tilde{\phi}^4/18$, with $h = 9\lambda_{k_0} m_{k_0}^2/\gamma_{k_0}^2$. For $h \approx 1$ the two minima of the potential have approximately equal depth, while for $h \to 0$ the metastable minimum at the origin has negligible depth compared to the stable one (spinodal point). One can estimate [4]

$$R = \frac{\ln \left(A_{k_0}/k_0^4 \right)}{S_{k_0}} \approx T(h)\, \frac{\lambda_{k_0}}{m_{k_0}}. \tag{3.2}$$

The function $T(h)$ diverges for $h \to 0$ [4], signalling the breakdown of homogeneous nucleation theory in the spinodal region. Moreover, this breakdown may occur even away from the spinodal region. $T(h)$ is small for h close to 1 [4], but a sufficiently large value of λ_{k_0}/m_{k_0} can lead to $R \gtrsim 1$. This case corresponds to weak first-order phase transitions, as can be verified by observing that the saddle-point action, the location of the true vacuum and the difference in free-energy density between the minima go to zero in the limit $m_{k_0}/\lambda_{k_0} \to 0$ for fixed h.

The above conclusions are confirmed by the numerical computation of the nucleation rate. A complete analysis of the region of validity of homogeneous nucleation theory for potentials of the form of eq. (2.1) was presented in ref. [4]. Also, two-scalar theories with potentials of various forms were studied in ref. [5]. The conclusions can be summarized as follows: Homogeneous nucleation theory relies on an expansion around the saddle point that is assumed to dominate the tunnelling process (the critical bubble). Therefore, it is applicable as long as this expansion converges. Its breakdown is signalled by a pre-exponential factor comparable to the leading exponential suppression and a strong dependence of the predicted nucleation rate on the coarse-graining scale.

[1] Models with $m_{k_0}^2 > 0$ and $m_{k_0}^2 < 0$ are related by a field shift [4]. We have employed this shift in order to move the metastable minimum to the origin in fig. 1.

4. Radiatively induced first-order phase transitions

These transitions [14] form a class of special interest, as many cosmological phase transitions belong to it. A typical example is presented in fig. 2 [5] for a two-scalar theory with an initial potential

$$U_{k_0}(\phi_1, \phi_2) = \frac{\lambda_{k_0}}{8} \left[(\phi_1^2 - \phi_{0k_0}^2)^2 + (\phi_2^2 - \phi_{0k_0}^2)^2 \right] + \frac{g_{k_0}}{4} \phi_1^2 \phi_2^2, \tag{4.1}$$

with $\phi_{0k_0}^2 = 1.712\ k_0$, $\lambda_{k_0} = 0.01\ k_0$ and $g_{k_0} = 0.2\ k_0$. In the first plot of the first row we depict a large part of the evolution of $U_k(\phi_1, \phi_2 = 0)$. The initial potential has only one minimum along the positive ϕ_1-axis and a maximum at the origin. In the sequence of potentials depicted by dotted lines we observe the appearance of a new minimum at the origin at some point in the evolution (at $k_{CW}/k_0 \approx e^{-4.4}$). This minimum is generated by the integration of fluctuations of the ϕ_2 field, whose mass depends on ϕ_1 through the last term in eq. (4.1) (the Coleman-Weinberg mechanism [14]). Immediately below we plot the mass term $\partial^2 U_k/\partial \phi_2^2(\phi_1, \phi_2 = 0)$ of the ϕ_2 field along the ϕ_1-axis. It turns positive at the origin at $k = k_{CW}$. We calculate the nucleation rate using the potentials of the last stages of the evolution. The solid lines correspond to $k_i/k_0 = e^{-4.7}$, while the line with longest dashes corresponds to $k_f/k_0 = e^{-5.2}$.

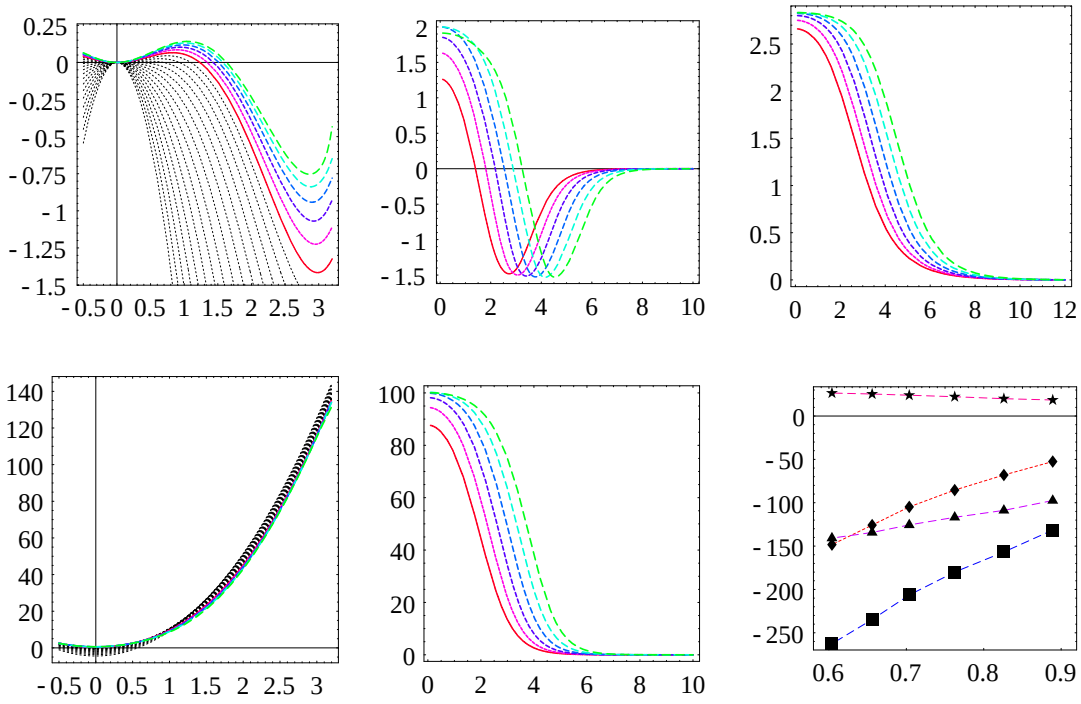

Figure 2: A radiatively induced first-order phase transition in a model with initial potential given by eq. (4.1) with $\phi^2_{0k_0} = 1.712\ k_0$, $\lambda_{k_0} = 0.01\ k_0$ and $g_{k_0} = 0.2\ k_0$. The calculation of the bubble-nucleation rate is performed between the scales $k_i = e^{-4.7} k_0$ and $k_f = e^{-5.2} k_0$. All dimensionful quantities are given in units of k_f.

In the third plot of the first row we display the profile of the saddle point $\phi_b(r)$ for various k between k_i and k_f. In the middle row we plot the quantities

$$W_{ik}(r) = \frac{\partial^2 U_k}{\partial \phi_i^2}\left(\phi_1 = \phi_b(r)\right) - \frac{\partial^2 U_k}{\partial \phi_i^2}\left(\phi_1 = 0\right) \tag{4.2}$$

for $\phi_2 = 0$ and $i = 1, 2$, i.e. the difference of the mass terms of the two fields along the bubble profile and the false vacuum. These quantities are expressed in units of k_f. We observe that the mass of the ϕ_2 fluctuations in the interior of the critical bubble is much larger than the other mass scales of the problem, which are comparable to k_f. This is a consequence of our choice of couplings $g_{k_0}/\lambda_{k_0} = 20$. Such a large ratio is necessary for a strong first-order phase transition to be radiatively induced.

The results for the nucleation rate are summarized in the last plot of the second row. The horizontal axis corresponds to the ratio of the scale k to the mass of the ϕ_1 field at the absolute minimum. The dark diamonds give the negative of the action of the saddle point $-S_k$ at the scale k. The stars indicate the values of the prefactor $\ln(A_{1k}/k_f^4)$ associated with ϕ_1 fluctuations, while the triangles denote the prefactor $\ln A_{2k}$ of the ϕ_2 field. A significant k dependence of all these quantities is observed. The dark squares give our results for $\ln(I/k_f^4) = -S_k + \ln[A_{1k} A_{2k}/k_f^4]$. This quantity has a strong k dependence, which signals the breakdown of the expansion around the saddle point. This is expected, as $|\ln A_{2k}|$ is comparable to the saddle-point action S_k, even though $\ln(A_{1k}/k_f^4)$ remains small.

The breakdown of the expansion is a generic problem of all the radiatively induced first-order phase transitions we have studied [5]. It can be understood in physical terms by considering the quantity $W_{2k}(r)$ defined in eq. (4.2) and depicted in the second plot of the second row in fig. 2. Due to the large values of the ratio $g_{k_0}/\lambda_{k_0} = 20$, the

mass of the ϕ_2 field is much larger than k_f, the typical scale of the tunnelling process. This indicates that fluctuations in the ϕ_2 direction cost excessive amounts of free energy and are suppressed. As these fluctuations are inherent to the system, the total nucleation rate should be suppressed as well. This explains the very negative values of $\ln A_{2k}$. This behaviour is not surprising. The radiative corrections to the potential and the pre-exponential factor have a very similar form of fluctuation determinants. When the radiative corrections are large enough to modify the initial potential and generate a new minimum, the pre-exponential factor should be expected to be important also.

We point out that the presence of a region of negative values for the function $W_{1k}(r)$, depicted in the second plot of the first row in fig. 2, results in the existence of a class of ϕ_1 fluctuations with small typical free energy. As a result, deformations of the critical bubble in the ϕ_1 direction are favourable and their effect tends to enhance the total nucleation rate. This explains the positive values of $\ln(A_{1k}/k_f^4)$.

Finally, we mention that the prefactor A_{2k} can be estimated using approximate expressions analogous to eq. (3.1) and appropriate rescalings. One finds [7]

$$\frac{\ln A_{2k_f}}{S_{k_f}} \approx -R(h)\,\frac{\lambda_{k_0}}{g_{k_0}}, \qquad (4.3)$$

with $R(h) \gtrsim 24$ for any h. This expression indicates that only very small values of λ_{k_0}/g_{k_0} may lead to a convergent expansion around the saddle point. However, eq. (4.3) is not valid for λ_{k_0} smaller than g_{k_0} by more than two orders of magnitude. We have not found any model for which the numerical study of a radiatively induced first-order phase transition indicates a convergent expansion.

5. Two dimensions

A crucial confirmation of the reliability of our approach was obtained in ref. [6], where bubble nucleation was studied for (2+1)-dimensional theories. Our results were compared with those of the lattice simulations of ref. [15]. We considered potentials similar to the one of eq. (2.1), with small modifications in order to match the continuum theory of the lattice simulations. The technical aspects of the application of our formalism to two dimensions can be found in ref. [6].

In fig. 3 we present a comparison of results obtained through our method with lattice results. The dimensionless parameter λ is approximately equal to $3\lambda_{k_0}/(\theta\, m_{k_0}^2)$ in terms of the parameters of the potential of eq. (2.1). The dimensionless variable θ (that plays the role of a rescaled temperature) is approximately equal to $\gamma_{k_0}^2/m_{k_0}^4$. The values of $1/\theta$ are given on the horizontal axis of the plots in fig. 3. (For the details, see ref. [6].) The diamonds denote the saddle-point action S_k. For every choice of λ, θ we determine S_k at two scales: $1.2\,k_f$ and $2\,k_f$. The light-grey region between the corresponding points gives an indication of the k dependence S_k. The negative of the bubble-nucleation rate $-\ln\left(I/m^3\right)$ is denoted by dark squares. The dark-grey region between the values obtained at $1.2\,k_f$ and $2\,k_f$ gives a good check of the convergence of the expansion around the saddle-point. If this region is thin, the prefactor is in general small and cancels the k dependence of the action. The dark circles denote the results for the nucleation rate from the lattice study of ref. [15].

For $\lambda = 0,\ 0.1,\ 0.2$ the values of $-\ln(I/m^3)$ computed at $1.2\,k_f$ and $2\,k_f$ are equal to a very good approximation. This confirms the convergence of the expansion around the saddle-point and the reliability of the calculation. The k dependence of the saddle-point action is cancelled by the prefactor, so that the total nucleation rate is k independent. Moreover, the prefactor is always significantly smaller than the saddle-point action. The agreement with the lattice predictions is good. It is clear that the contribution of the prefactor is crucial for the correct determination of the total bubble-nucleation rate.

For larger values of λ the matching between the lattice and the renormalized actions becomes imprecise. As a result, we cannot make sure that we are studying the same theory as the one simulated on the lattice. This generates deviations of our results from the lattice ones, which start becoming apparent for $\lambda = 0.25$. However, the internal consistency criteria of our method provide a test of the convergence of the expansion around

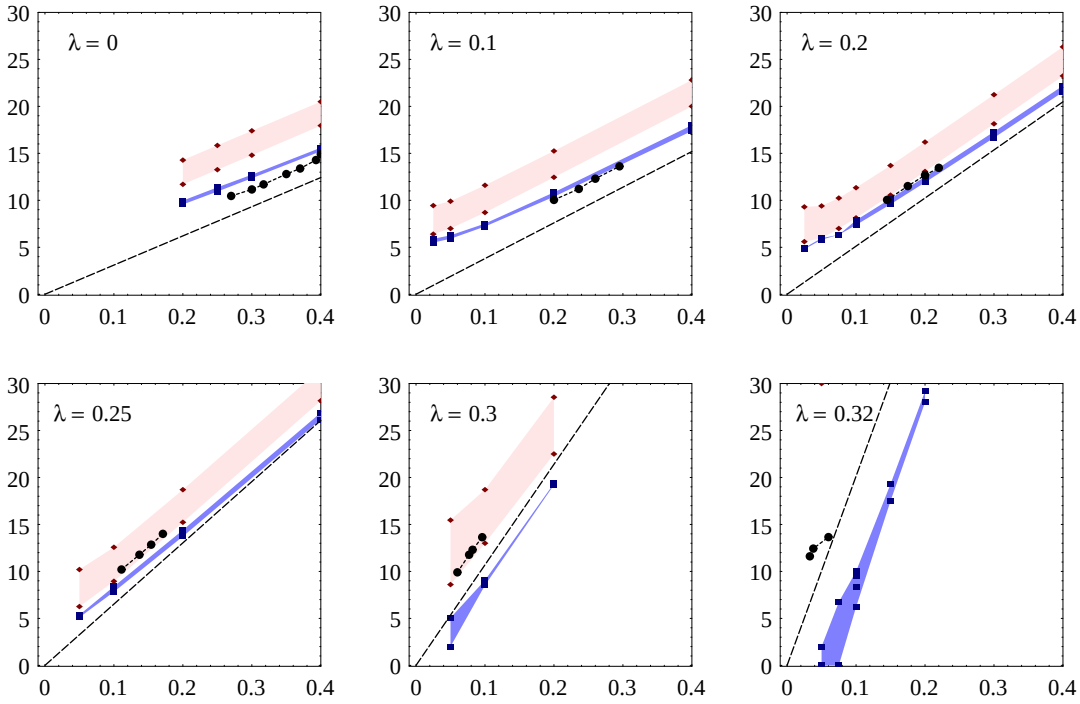

Figure 3: Comparison of our method with lattice studies: Diamonds denote the saddle-point action S_k and squares the bubble-nucleation rate $-\ln\left(I/m^3\right)$ for $k = 1.2\,k_f$ and $2\,k_f$. Dark circles denote the results for the nucleation rate from the lattice study of ref. [15].

the saddle point in all cases. The consistency of our calculation is achieved for $1/\theta \gtrsim 0.12$ even for $\lambda = 0.32$. However, the breakdown of the expansion is apparent for $1/\theta \lesssim 0.12$. The prefactor becomes comparable to the saddle-point action and the k dependence of the predicted nucleation rate is strong.

6. Applications

As a first example we consider the bound on the Higgs-boson mass from the stability of our vacuum. The top-quark radiative corrections to the zero-temperature effective potential of the Higgs field may result in the appearance of a new minimum, deeper than the one located at 247 GeV. In order for this not to happen, a lower bound on the Higgs-boson mass must be imposed. This bound can be relaxed if one allows for the presence of a new vacuum, but demands that the time needed for a transition to it is larger than the age of our universe. The largest rates are associated with thermal transitions at high temperatures, from a metastable minimum in the symmetric phase of the Standard Model directly to the absolute minimum at very large Higgs-field expectation values [16].

We consider the effective three-dimensional description of the top-Higgs system at a scale $k_0 \approx T$. The top-quark fluctuations are almost decoupled because of the absence of a zero Matsubara frequency for fermions. This permits a very simple determination of the potential $U_{k_0}(\phi)$, which is equal to the sum of the zero-temperature potential and the contribution from the top-quark thermal fluctuations [7]. It can be written as

$$U_{k_0}(\phi) \approx \frac{m^2}{2}\phi^2 - \frac{\kappa}{4}\phi^4, \qquad (6.1)$$

where $m^2 = g_{t4}^2\,T^2/4$, $\kappa = |\lambda_4|\,T$, g_{t4} is the top-quark Yukawa coupling and λ_4 the average (negative) value of the quartic coupling over the region of Higgs-field expectation values relevant for the critical-bubble profile. The term $\sim \phi^2$ is the leading temperature correction in the expansion of the one-loop contribution from the top quark.

The action of the saddle point is [7]

$$S_{k_0} \approx 18.9 \frac{m}{\kappa} = 9.45 \, \frac{g_{t4}}{|\lambda_4|}. \qquad (6.2)$$

The prefactor can be estimated through eq. (3.2)

$$\ln \left(A_{k_0} / k_0^4 \right) \approx 2.00 \, \frac{k_0 \, \pi}{2 \, m} = \frac{6.28}{g_{t4}}. \qquad (6.3)$$

For the experimental value of the top-quark mass ($g_{t4} \approx 1$) we find $|\lambda_4| \lesssim 0.05$ for all Higgs-field expectation values, in agreement with ref. [16]. As a result, the prefactor is expected to give only a small correction to the bubble-nucleation rate.

The electroweak phase transition is radiatively induced by gauge field fluctuations. Even though the generalization of our formalism to gauged systems requires further work, an estimate of the validity of the expansion around the saddle point can be obtained by exploiting the resemblance between the gauge-field fluctuation determinants and the ones in two-scalar models. The estimate for the prefactor $|\ln A_{2k_f}|$, associated with the gauge fields, is given by eq. (4.3), with λ/g taking the "effective" value [7]

$$\left(\frac{\lambda}{g} \right)_{\rm SM} \approx \frac{(4m_W + 2m_Z) \, m_H^2}{4(4m_W^3 + 2m_Z^3)} = 0.35 \, \left(\frac{m_H}{100 \, {\rm GeV}} \right)^2. \qquad (6.4)$$

For the prefactor to be smaller than 1/2 of the action, $m_H \lesssim 25$ GeV is required.

Higgs-boson masses below the experimental lower limit of 90 GeV are of academic interest. Moreover, for $m_H \gtrsim 80$ GeV, there is no phase transition in the high-temperature Standard Model. There is the possibility, however, for a sufficiently strong first-order phase transition for baryogenesis within the Minimal Supersymmetric Standard Model with a very light stop [17]. In this model, the "effective" value of g/λ obeys [7]

$$\left(\frac{\lambda}{g} \right)_{\rm MSSM} \gtrsim \frac{(4m_W + 2m_Z + 6m_t) \, m_H^2}{4(4m_W^3 + 2m_Z^3 + 6m_t^3)} = 0.11 \, \left(\frac{m_H}{100 \, {\rm GeV}} \right)^2. \qquad (6.5)$$

For $m_t = 175$ GeV, in order to have a prefactor smaller than 1/2 of the action, $m_H \lesssim 45$ GeV is required.

References

[1] J. Langer, *Ann. Phys. (NY)* **41** (1967) 108; *ibid.* **54** (1969) 258; *Physica* **73** (1974) 61.

[2] S. Coleman, *Phys. Rev.* **D 15** (1977) 2929; C.G. Callan and S. Coleman, *Phys. Rev.* **D 16** (1977) 1762; I. Affleck, *Phys. Rev. Lett.* **46** (1981) 388; A.D. Linde, *Nucl. Phys.* **B 216** (1983) 421.

[3] A. Strumia and N. Tetradis, *Nucl. Phys.* **B 542** (1999) 719 [hep-ph/9806453].

[4] A. Strumia, N. Tetradis and C. Wetterich, hep-ph/9808263.

[5] A. Strumia and N. Tetradis, to appear in *Nucl. Phys.* **B** [hep-ph/9811438].

[6] A. Strumia and N. Tetradis, hep-ph/9904246.

[7] A. Strumia and N. Tetradis, hep-ph/9904357.

[8] J. Berges, N. Tetradis and C. Wetterich, *Phys. Lett.* **B 393** (1997) 387 [hep-ph/9610354]; J. Berges and C. Wetterich, *Nucl. Phys.* **B 487** (1997) 675 [hep-th/9609019].

[9] C. Wetterich, *Nucl. Phys.* **B 352** (1991) 529; *Z. Physik* **C 57** (1993) 451; *ibid.* **60** (1993) 461.

[10] C. Wetterich, *Phys. Lett.* **B 301** (1993) 90.

[11] N. Tetradis and C. Wetterich, *Nucl. Phys.* **B 422** (1994) 541 [hep-ph/9308214]; T.R. Morris, *Phys. Lett.* **B 329** (1994) 241 [hep-ph/9403340].

[12] N. Tetradis and C. Wetterich, *Nucl. Phys.* **B 398** (1993) 659; *Int. J. Mod. Phys.* **A 9** (1994) 4029 [hep-ph/9309257]; N. Tetradis, *Nucl. Phys.* **B 488** (1997) 92 [hep-ph/9608272].

[13] A. Ringwald and C. Wetterich, *Nucl. Phys.* **B 334** (1990) 506; N. Tetradis and C. Wetterich, *Nucl. Phys.* **B 383** (1992) 197.

[14] S. Coleman and E. Weinberg, *Phys. Rev.* **D 7** (1973) 1888.

[15] M. Alford and M. Gleiser, *Phys. Rev.* **D 48** (1993) 2838 [hep-ph/9304245].

[16] G. Anderson, *Phys. Lett.* **B 243** (1990) 265; P. Arnold and S. Vokos, *Phys. Rev.* **D 44** (1991) 3620; J.R. Espinosa and M. Quirós, *Phys. Lett.* **B 353** (1995) 257 [hep-ph/9504241].

[17] M. Carena, M. Quiros and C. Wagner, *Phys. Lett.* **B 380** (1996) 81 [hep-ph/9603420]; M. Carena, M. Quiros, A. Riotto, I. Vilja and C. Wagner, *Nucl. Phys.* **B 503** (1997) 387 [hep-ph/9702409].